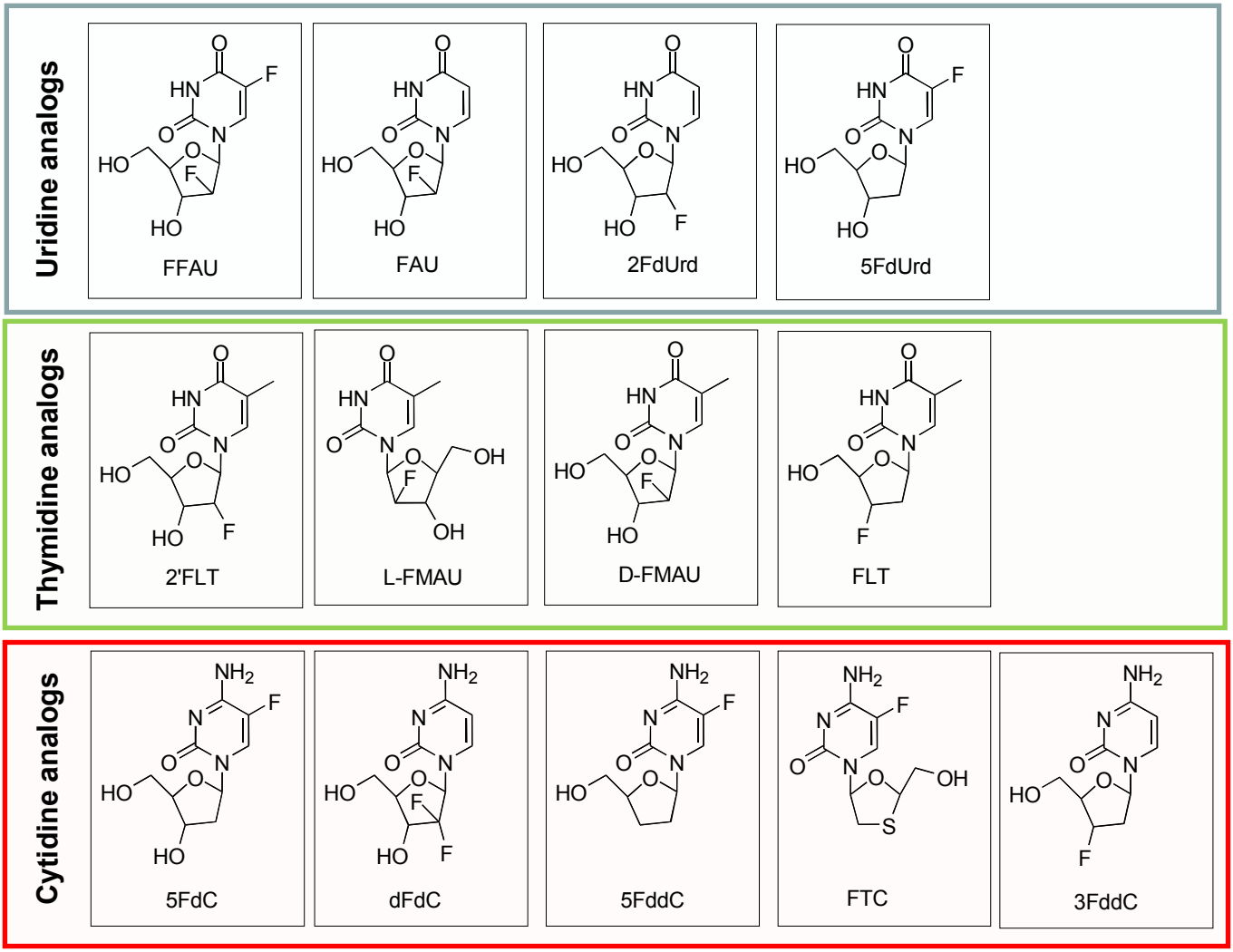

Uridine analogs	
2'-Fluoro-2'-deoxy 5-Fluorouracil-β-D-arabinofuranoside	FFAU
1-(2-deoxy-2-fluoro-B-D-arabinofuranosyl)-uracil	FAU
2'-Fluoro-2-deoxyuridine	2FdUrd
5-Fluoro-2-deoxyuridine	5FdURD
Thymidine analogs	
2' Fluoro 2' deoxyThymidine	2'FLT
1-(2-Deoxy-2-Fluoro-B-L-arabinofuranosyl) 5 methyluracil	L-FMAU
1-(2-Deoxy-2-Fluoro-B-D-arabino-furanosyl)-5-methyluracil	D-FMAU
3' Fluoro 3' deoxyThymidine	FLT
Cytidine analogs	
5-Fluoro-2'-Deoxycytidine	5FdC
2',2'-Difluorodeoxycytidine	dFdC
5-Fluoro-2,3-dideoxycytidine	5FddC
(-)-β-2,3-Dideoxy-5-fluoro-3-thiacytidine	FTC
2,3-dideoxy-3-fluorocytidine	3FddC

Supplementary Figure 1. Fluorinated deoxyribonucleoside analogs used in this paper.

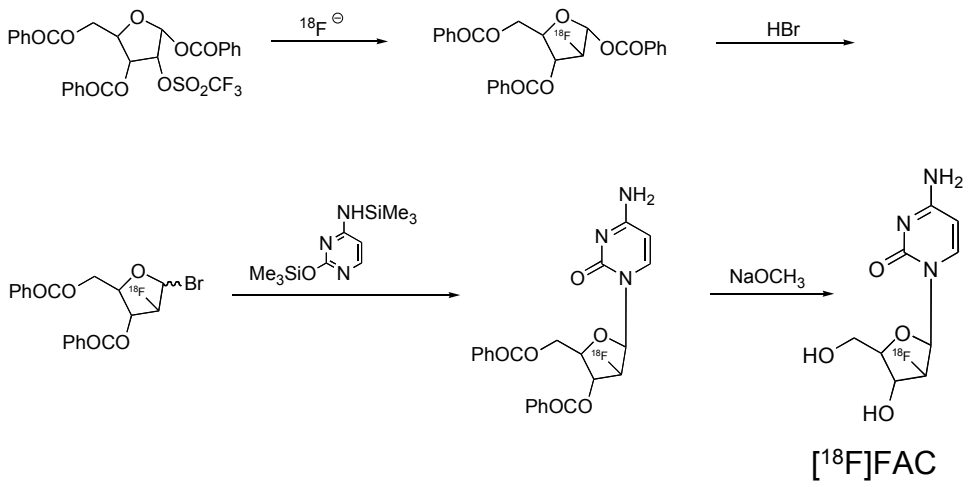

Supplementary Figure 2. Radiochemical synthesis of [^{18}F]FAC. 1-Bromo-2-[^{18}F]Fluoro-3,5-di-O-benzoyl-D-arabinofuranose was prepared as reported in the literature 40. This ^{18}F-labeled sugar derivative was reacted with a freshly prepared trimethylsilyl protected derivative of cytosine in dichloroethane. The resultant intermediate analog was then treated with a solution of sodium methoxide in methanol to remove the benzoyl protecting groups. The crude reaction product was purified by semi-preparative HPLC (Phenomenex Gemini C-18 column; 25 cm X 1 cm). The column was eluted with a solvent mixture of 1% ethanol and 99% 10 mM ammonium dihydrogen phosphate at a flow rate of 5.0 mL/min. The effluent from the column was monitored with a 254 nm UV detector followed by a gamma radioactive detector. The chemically and radiochemically pure [^{18}F]FAC eluted off the column with a retention time of ~15 min and the radiochemical yield ranged between 20 and 30%. The product isolated from semi-preparative HPLC was made isotonic with sodium chloride and sterilized by passing through a Millipore filter (0.22 μm) into a sterile multi-dose vial.

a

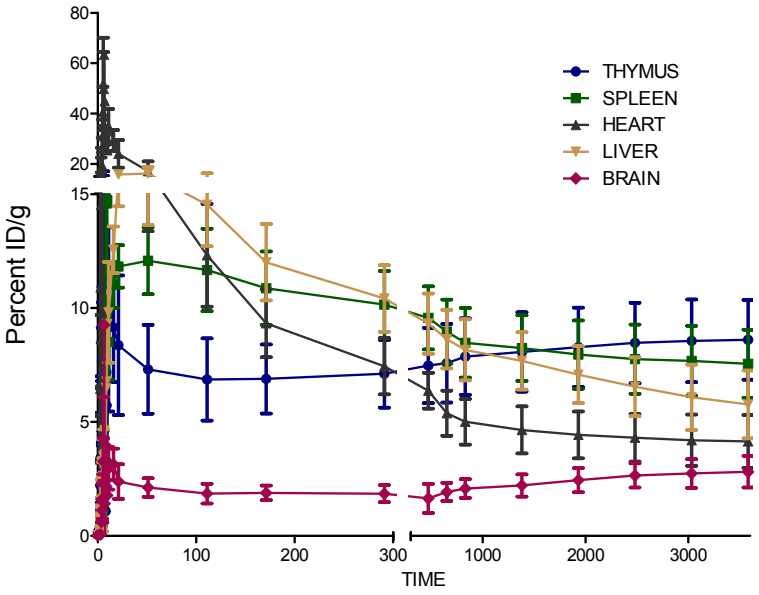

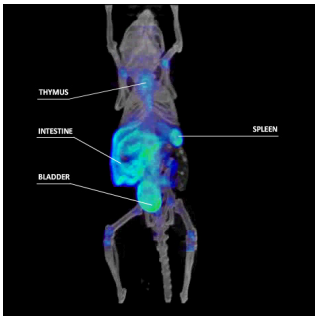

b (see Supplementary Fig 3b online movies)

c

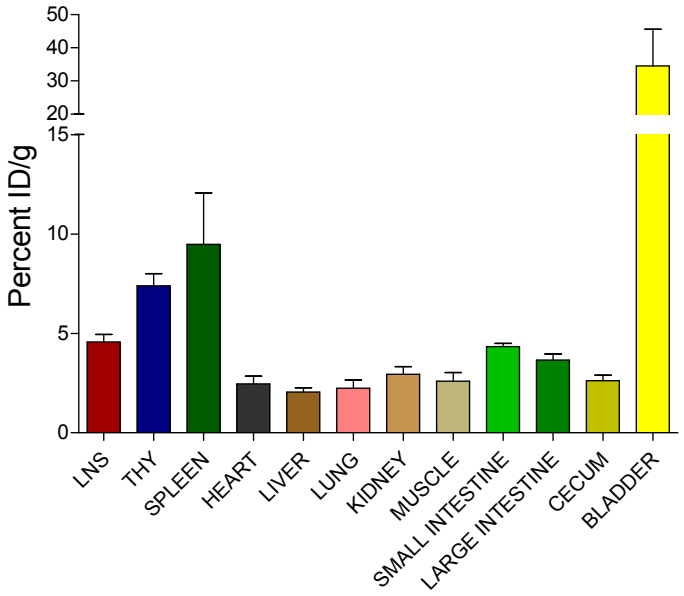

Supplementary Figure 3. Biodistribution of [^{18}F]FAC. (a) Decay-corrected mean time-activity curves in various organs of normal mice injected with [^{18}F]FAC. **(b) see Supplementary Fig 3b online movies)** Shown is a mouse microPET dynamic image set taken over the course of 60 min after injection of [^{18}F]FAC via tail-vein. At 0-3 min [^{18}F]FAC quickly distributes out of blood and is cleared via the kidney into the bladder. At 3-60 min the [^{18}F]FAC is retained in the spleen, thymus and small and large intestine. **(c)** [^{18}F]FAC biodistribution measured on necropsy tissue samples 60 min after i.v. injection of the probe.

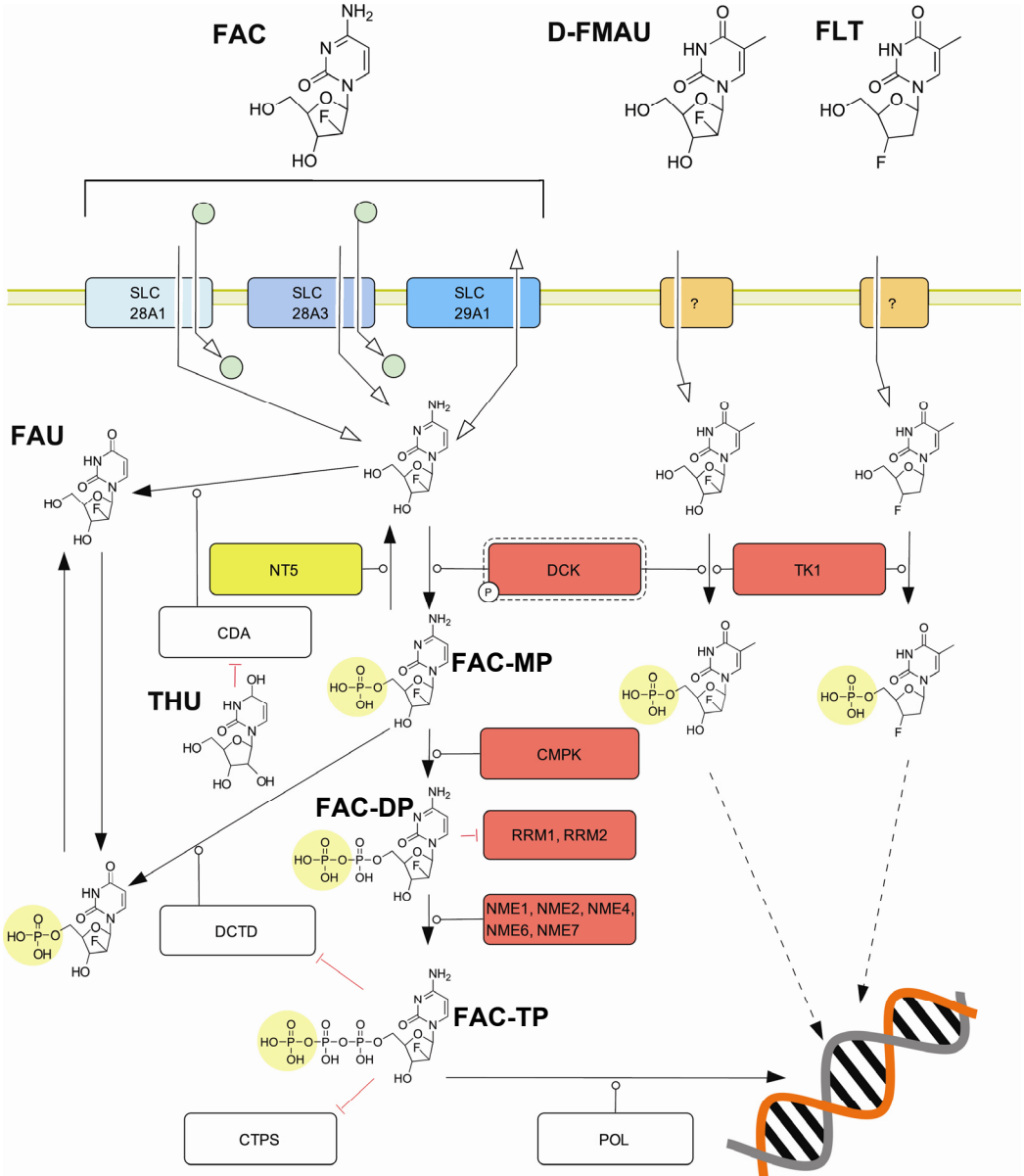

Supplementary Figure 4. Potential metabolic pathways for [^{18}F]FAC and other ^{18}F labeled PET probes (D-FMAU and FLT) for the nucleoside salvage pathway. Putative transporters for FAC include the solute carriers SLC28A1, SLC28A3 and SLC29A1. Among these, only SLC29A1 is expressed at the mRNA level in naïve and proliferating T lymphocytes. The precise identity of lymphocyte-expressed nucleoside transporters specific for TK1 substrates D-FMAU and FLT is uncertain. Intracellularly, FAC is phosphorylated by deoxycytidine kinase (dCK). FAC can also be converted to its uracil metabolite FAU by cytidine deaminase (CDA). CDA can be inhibited by 3,4,5,6-tetrahydrouridine (THU). Monophosphorylated FAC (FAC-MP) is a potential substrate for cytidylate kinase (CMPK) and deoxycytidylate deaminase (DCTD). Diphosphorylated FAC (FAC-DP) is a potential substrate for nucleoside diphosphate kinases (NME1, NME2, NME4, NME6, NME7). FAC-DP can inhibit ribonucleotide reductase (RRM) and triphosphorlayed FAC (FAC-TP) can inhibit DCTD and cytidine triphosphate synthase (CTPS). FAC-TP may then be incorporated into DNA via DNA polymerase (POL). D-FMAU and FLT are phosphorylated by thymidine kinase 1 (TK1). D-FMAU is also a substrate for dCK. EC (Enzyme Commission) numbers for the key enzymes involved in the nucleoside salvage pathway are as follows: CDA (3.5.4.5), CMPK (2.7.4.14), CTPS (6.3.4.2), dCK (2.7.1.74), DCTD (3.5.4.12), 2.7.4.6 (NME1, NME2, NME4, NME6, NME7), 3.1.3.5 (NT5), 2.7.7.7 (POL), 1.17.4.1 (RRM), and 2.7.1.21 (TK1).

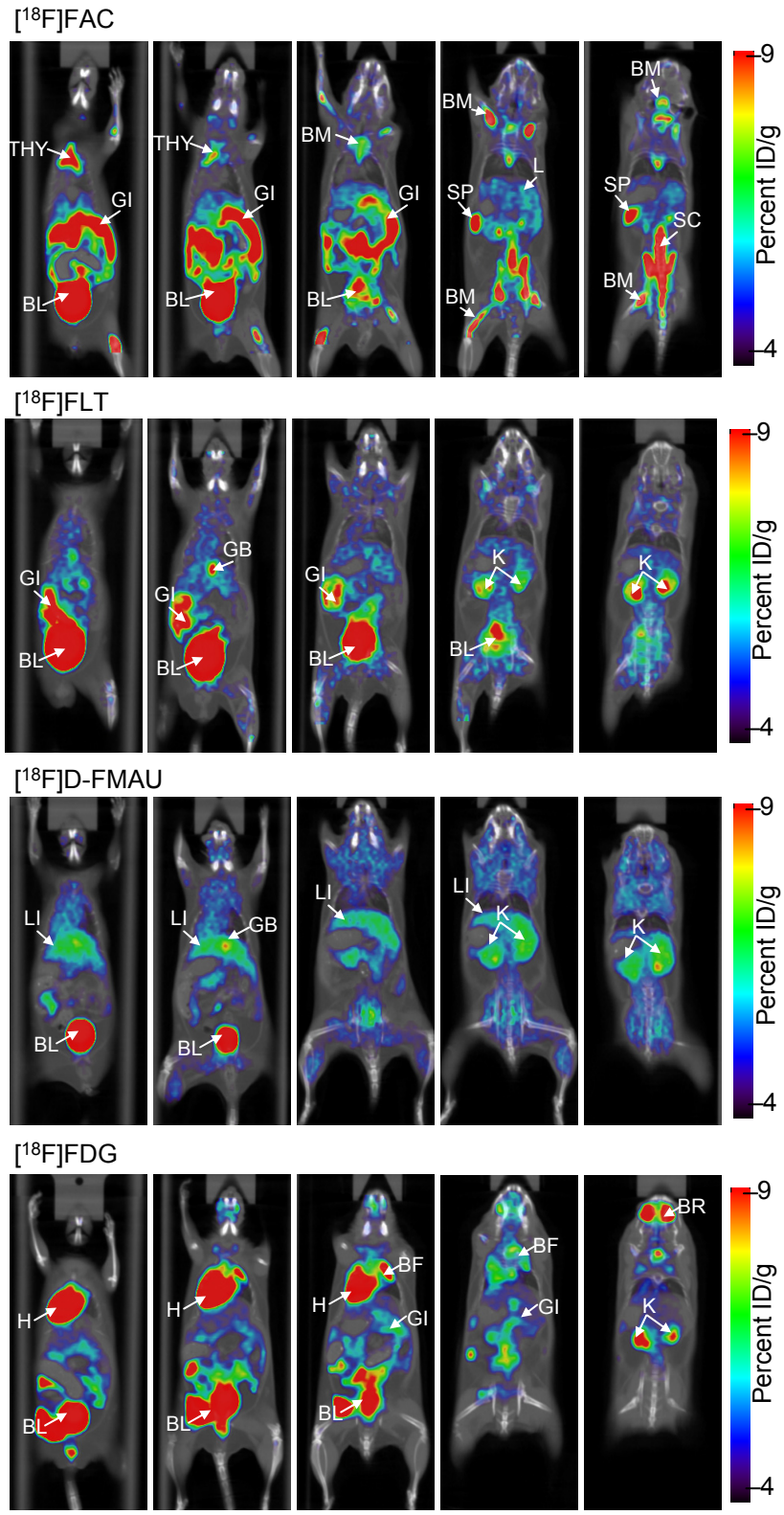

Supplementary Figure 5. [^{18}F]FAC has better selectivity for lymphoid organs compared with other PET probes for nucleoside metabolism and glycolysis. C57/BL6 mice were scanned by microPET/CT using [^{18}F]FAC, [^{18}F]FLT, [^{18}F]D-FMAU and [^{18}F]FDG. Mice were imaged 60 min after i.v. injection of probes. Images are 2 mm thick coronal slices anterior to posterior. Percent ID/g, percent injected dose per gram of tissue; BM, Bone-marrow; BL, Bladder; BR, Brain; GB, Gall Bladder; GI, Gastrointestinal tract; H, heart; K, Kidney; L, Liver; LU, Lung; SP, Spleen; Thy, thymus; BF, brown fat. See Fig. 2 for details.

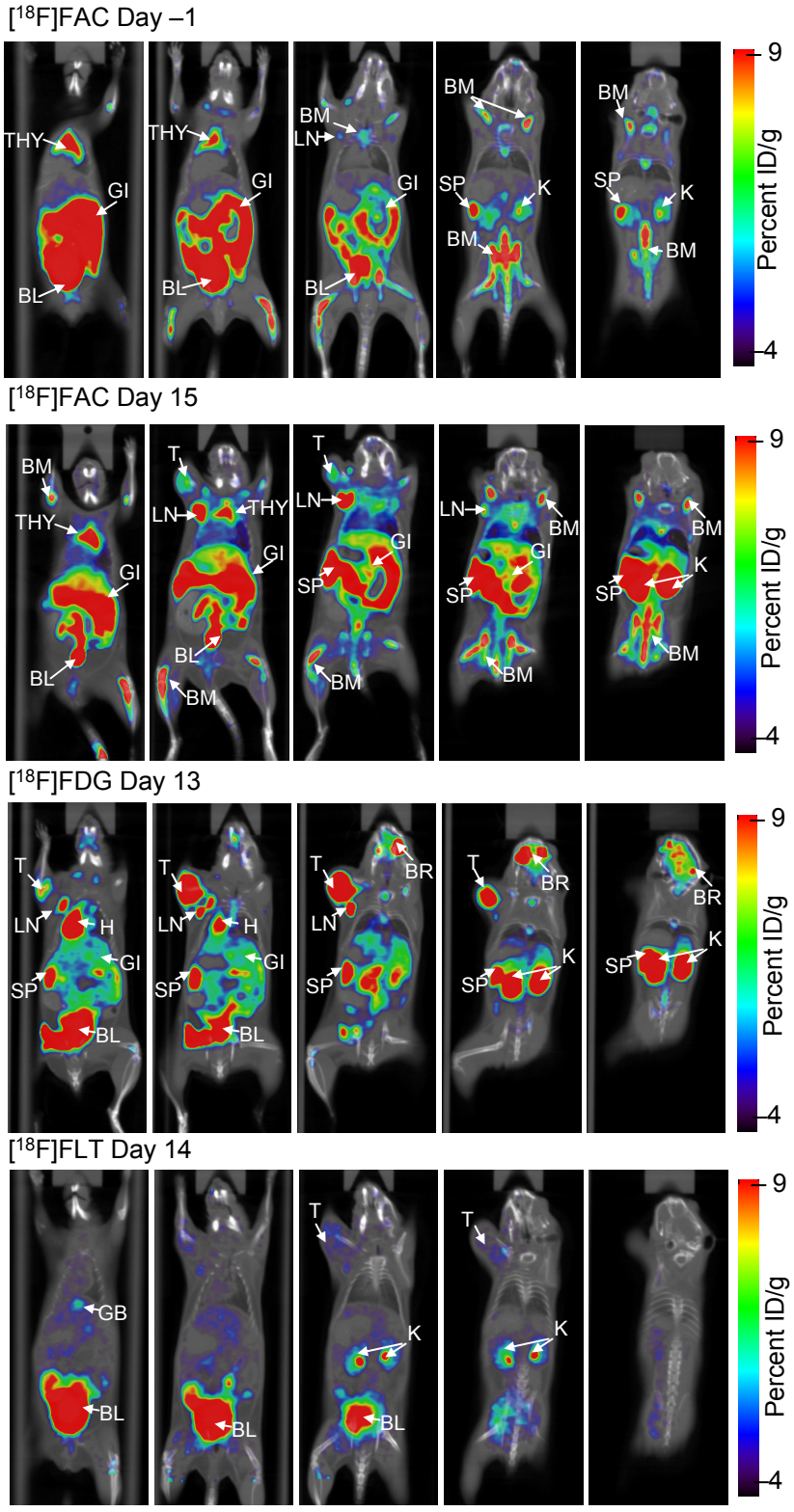

Supplementary Figure 6. Increased [^{18}F]FAC retention in spleen and lymph nodes at the peak of the primary anti-tumor immune response. Images are 2 mm coronal sections anterior to posterior from microPET/CT scans using [^{18}F]FAC (Day –1 and Day 15), [^{18}F]FDG (Day 13) and [^{18}F]FLT (Day 14). B, Bone; BL, Bladder; GI, Gastrointestinal tract; H, heart; SP, Spleen; TU, tumor; Thy, thymus; LN, lymph node. See Fig. 3 for details.

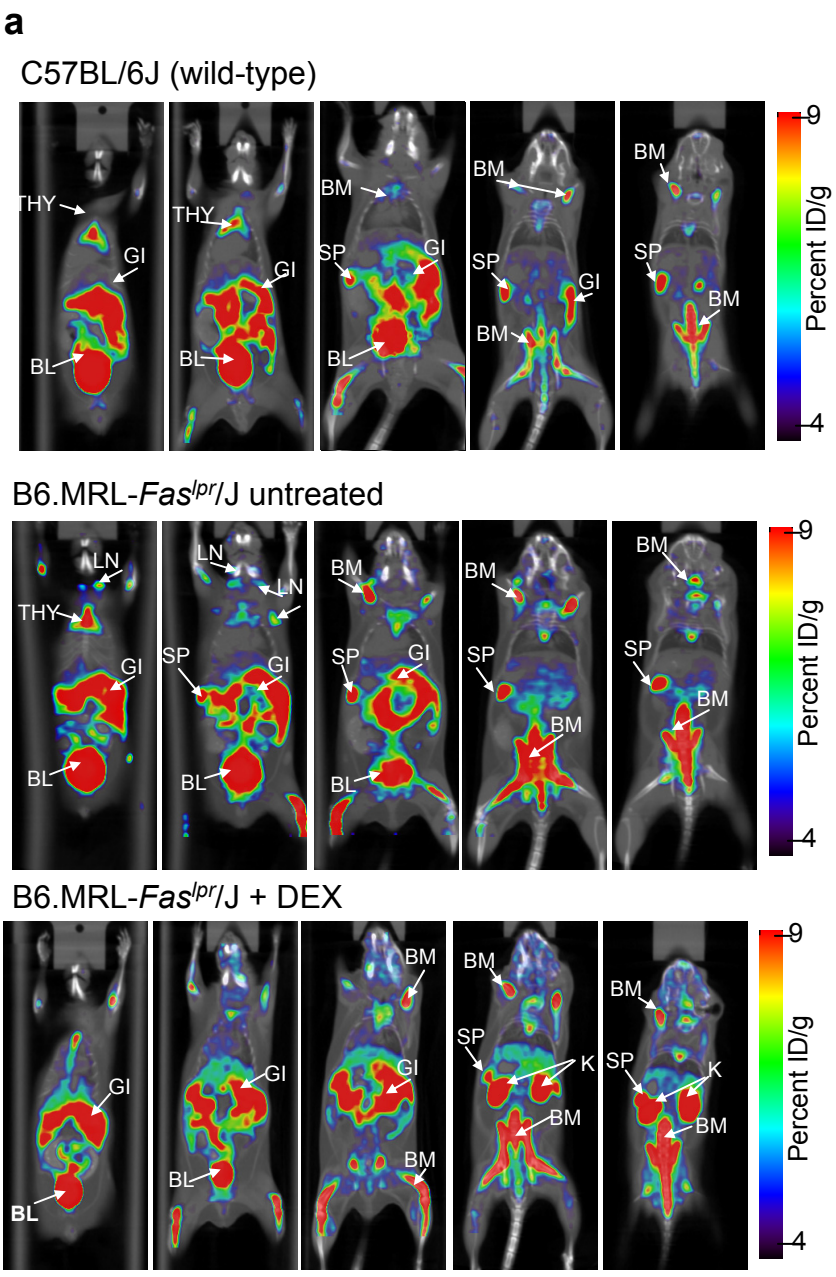

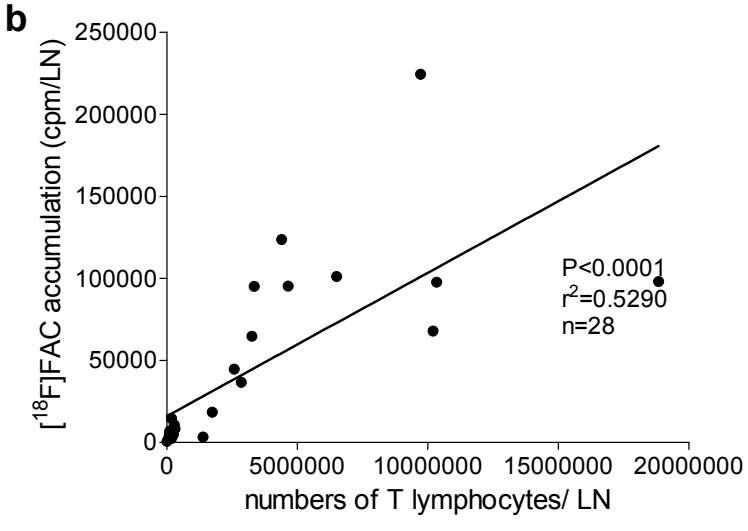

Supplementary Figure 7. [^{18}F]FAC microPET/CT allows visualization of increased lymphoid mass in systemic autoimmunity and can be used to monitor immunosuppressive therapeutic interventions. **(a)** Images are 60 minutes after i.v. injection of [^{18}F]FAC and show five 2 mm thick whole body coronal slices from wild-type (C57BL/6J) and B6.MRL-*Faslpr*/J before and after treatment with DEX. Thy, thymus; LN, lymph nodes; BM, bone marrow. See Fig. 4 for details. **(b)** The amount of [^{18}F]FAC radioactivity retained in lymph nodes from the B6.MRL-*Faslpr*/J mice correlates with the number of lymphocytes at these sites.

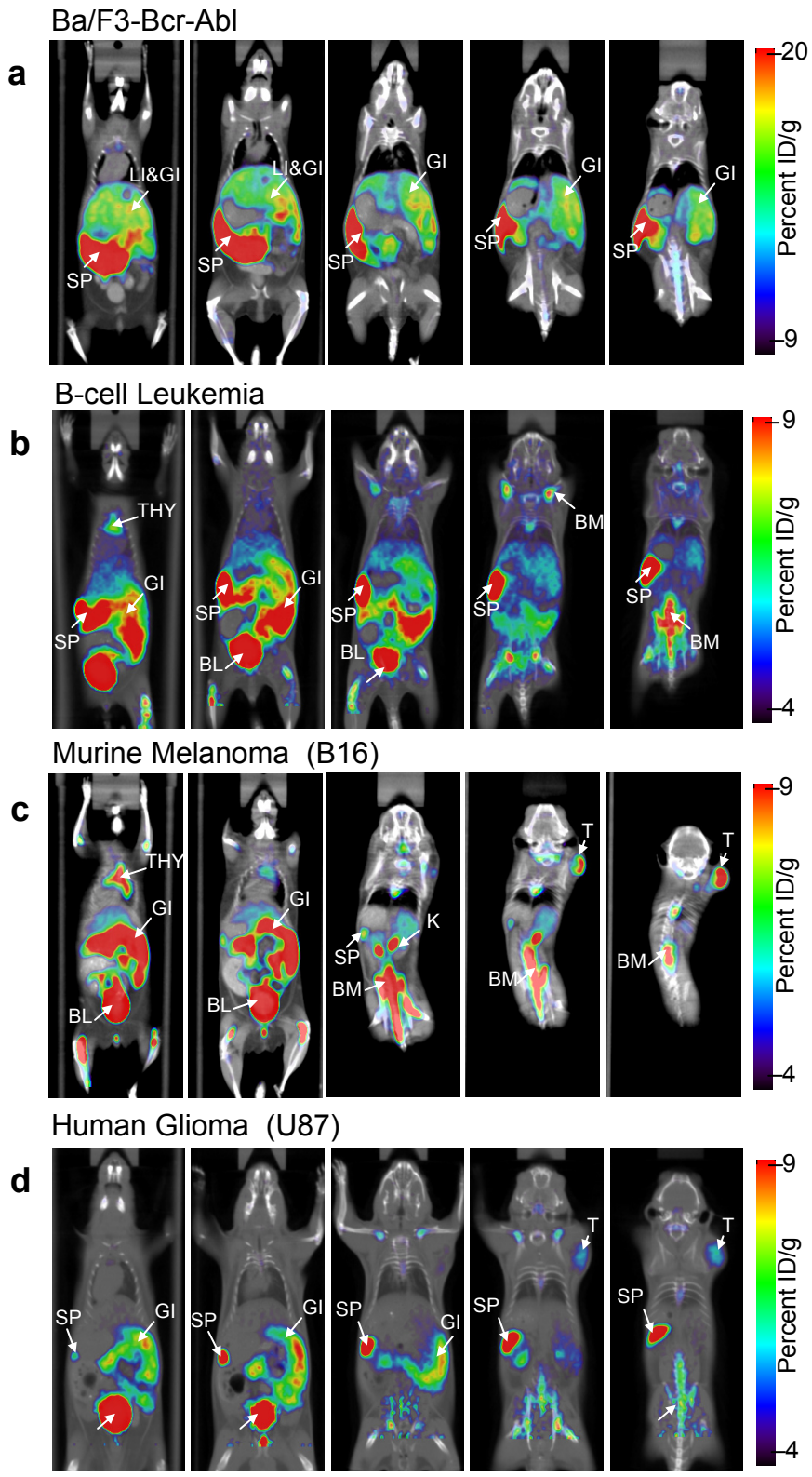

Supplementary Figure 8. [^{18}F]FAC microPET/CT imaging of human and murine tumors. Images are 2 mm coronal sections from [^{18}F]FAC microPET/CT scans 1 hr after probe injection. **(a)** SCID mice were injected intravenously with Ba/F3 cells expressing p210 BCR-ABL. Mice develop aggressive disease, with massive splenic infiltration, typically resulting in death in ~15 days. Mice were imaged on day 12 following injection. **(b)** NOD SCID mice were transplanted with wild-type total bone marrow cells infected with MSCV-GFP-IRES-P185 BCR-ABL retroviral stocks. Leukemic mice were imaged 28 days following transplantation. **(c)** C57BL/6 were injected s.c. with 1 x 10^5 B16 melanoma cells and imaged 7 days later. **(d)** SCID mice were injected s.c. with 1 x 10^6 U87 glioma cells and imaged 10 days later. L, Liver; SP, Spleen; GI, Gastrointestinal tract; BL, Bladder; Tu, Tumor.

Molecular imaging of lymphoid organs and immune activation using positron emission tomography with a new ^{18}F-labeled 2'-deoxycytidine analog

Caius G. Radu[1,2], Chengyi J. Shu[3], Evan Nair-Gill[1], Stephanie M. Shelly[1], Jorge R. Barrio[1], Nagichettiar Satyamurthy[1], Michael E. Phelps[1,2], and Owen N. Witte[1,3,4]

SUPPLEMENTARY METHODS

Microarray gene expression analyses. Total RNA was extracted from purified naïve and proliferating (72 hrs post activation) CD8+ T cells from the pmel-1 TCR transgenic mice. Pooled RNA from 4 independent experiments was hybridized to Affymetrix Mouse Genome 430 2.0 arrays. Absolute calls describing whether a probe set is present (P), marginally present (M), or absent (A) were generated using the Affymetrix GeneChip Operating Software v1.3 (GCOS) and expression values were calculated using the PM/MM difference model of DNA-Chip (dChip) [1]. Expression values across samples were normalized using dChip's invariant set method. A gene was considered differentially expressed if the corresponding probe set fit the following criteria: absolute call was P in at least half of the samples, fold change >1.4 between baseline (naïve CD8+ T cells) and experimental (activated CD8+ T cells) using the lower 90% confidence bound of fold change as defined in dChip [1], and expression difference between the baseline and experimental samples was >100. Genes involved in the nucleoside de novo biosynthesis and salvage pathways were taken from the KEGG database [2] (pathway IDs 00230 and 00240), and corresponding probe sets were manually extracted from Affymetrix's NetAffx [3] to ensure complete coverage of all nucleoside pathway genes (239 probe sets), plus the SLC28 and SLC29 transporters (10 probe sets). The complete dataset has been deposited in the public Gene Expression Omnibus (GEO) Database under accession number GSE9997.

Quantitative Real-Time PCR gene expression analysis (qPCR). Total RNA was purified from tissues using the Qiagen RNeasy Mini kit. 1.5 µg of RNA was then used to synthesize cDNA using the TaqMan Reverse Transcription Reagents (Applied Biosystems). Pre-designed TaqMan assays were purchased from Applied Biosystems for dCK (Assay ID: Mm00432794_m1), Slc29a1 (Assay ID: Mm00452176_m1), and Slc28a3 (Assay ID: Mm00627874_m1). TaqMan β-actin (Applied Biosystems, Part: 4352341E) reagents were used

as an endogenous control for quantification. The samples were run on a 48-well StepOne Real-Time PCR System (Applied Biosystems) and were analyzed with the StepOne Software v2.0 (Applied Biosystems) using the comparative Ct method ($\Delta\Delta$Ct). The qPCR mixture (20 µL) contained 15 ng cDNA, TaqMan buffer, 5.5 mM $MgCl_2$, 200 µM dATP, 200 µM dCTP, 200 µM dGTP, 400 µM dUTP, the appropriate TaqMan assay, 0.5U AmpliTaq Gold, and 0.2U uracil-N-glycosylase (UNG). Each assay included cDNA template in triplicates.

Biodistribution studies. Animals were anesthetized with 2% isoflurane, injected i.v. with 200 µCi [^{18}F]FAC and scanned with microPET/CT. Mice were sacrificed immediately after imaging. Organs were rapidly excised, weighed and the radioactivity was measured in a well counter. After decay correction, results were expressed as percent of the injected dose of activity per gram of tissue (%ID/g).

In vivo **leukemogenesis assay.** 6-8 week old severe combined immunodeficient (NOD SCID) mice were sublethally irradiated (275 rads) one day prior to reconstitution. Whole bone marrow were isolated from the tibias and femurs of 4-8 week old wild-type mice and infected with the MSCV-GFP-IRES-P185 BCR-ABL retrovirus. Three hours after infection, bone marrow cells were injected intravenously by tail vein into recipient NOD SCID mice. Animals were monitored daily for signs of illness for two months as previously described [4].

Cell lines. p210 BCR-ABL transfected Ba/F3 cell lines were previously described [5] and were maintained in RPMI containing 10% FCS in 5% CO_2 at 37°C with the addition of 10% WEHI conditioned medium as a source of IL-3. B16 (H-2^b), a spontaneous gp100$^+$ murine melanoma and the U87 glioma cell line were obtained from the American Type Culture Collection (ATCC, Rockville, MD).

SUPPLEMENTARY METHODS REFERENCES

1. Li, C. & Wong, W.H. Model-based analysis of oligonucleotide arrays: expression index computation and outlier detection. *Proc Natl Acad Sci U S A* **98**, 31-36 (2001).
2. Kanehisa, M. & Goto, S. KEGG: kyoto encyclopedia of genes and genomes. *Nucleic acids research* **28**, 27-30 (2000).
3. Liu, G.*, et al.* NetAffx: Affymetrix probesets and annotations. *Nucleic acids research* **31**, 82-86 (2003).
4. Afar, D.E.*, et al.* Regulation of the oncogenic activity of BCR-ABL by a tightly bound substrate protein RIN1. *Immunity* **6**, 773-782 (1997).

5. Ahmed, M.*, et al.* BCR-ABL and constitutively active erythropoietin receptor (cEpoR) activate distinct mechanisms for growth factor-independence and inhibition of apoptosis in Ba/F3 cell line. *Oncogene* **16**, 489-496 (1998).